Improvements on radiative acceleration calculations in stellar envelopes

Jean-François Gonzalez, Francis Leblanc, Marie-Christine Artru, Georges Michaud

▶ **To cite this version:**

Jean-François Gonzalez, Francis Leblanc, Marie-Christine Artru, Georges Michaud. Improvements on radiative acceleration calculations in stellar envelopes. Astronomy and Astrophysics - A&A, 1995, 297, pp.223. hal-03985523

HAL Id: hal-03985523
https://hal.science/hal-03985523

Submitted on 13 Feb 2023

HAL is a multi-disciplinary open access archive for the deposit and dissemination of scientific research documents, whether they are published or not. The documents may come from teaching and research institutions in France or abroad, or from public or private research centers.

L'archive ouverte pluridisciplinaire **HAL**, est destinée au dépôt et à la diffusion de documents scientifiques de niveau recherche, publiés ou non, émanant des établissements d'enseignement et de recherche français ou étrangers, des laboratoires publics ou privés.

Distributed under a Creative Commons Attribution 4.0 International License

1995A&A...297..223G

Astron. Astrophys. 297, 223–236 (1995)

ASTRONOMY AND ASTROPHYSICS

Improvements on radiative acceleration calculations in stellar envelopes

J.-F. Gonzalez[1], F. LeBlanc[2,3,4], M.-C. Artru[1,5], and G. Michaud[3,4]

[1] Ecole Normale Supérieure de Lyon, Laboratoire de Physique (CNRS-URA 1325), 46 allée d'Italie, F-69364 Lyon Cédex 07, France
[2] Département de Physique, Université de Moncton, Moncton, N.-B., E1A 3E9, Canada
[3] CEntre de Recherche en Calcul Appliqué, 5160 boul. Décarie, bureau 400, Montréal, Québec, H3X 2H9, Canada
[4] Département de Physique, Université de Montréal, Case Postale 6128, Succursale A, Montréal, Québec, H3C 3J7, Canada
[5] Observatoire de Lyon (CNRS-URA 300), 9 avenue Charles André, F-69561 Saint-Genis Laval Cédex, France

Received 12 July 1994 / Accepted 11 October 1994

Abstract. The various processes that need to be included in calculations of radiative acceleration in stellar envelopes are presented and their importance is evaluated. The general procedure used to compute radiative accelerations and the usual approximations are recalled, together with a summary of the useful equations.

Major improvements are obtained by using the newly available atomic data provided by the OPACITY project (OP). They first allow to compute the frequency dependence of the background opacity and to improve the evaluation of the collisional line broadening. The contributions of bound-bound and bound-free transitions to the radiative acceleration are then calculated for each ion of a given element. A method of averaging among ions is developed to obtain the net acceleration on the element, in a simple model taking into account the effects of rapid reactions between ions.

Examples of results are given for carbon and iron in a model-envelope with $T_{\rm eff}$ = 8000 K, $\log g$ = 4.2, Z = 0.02. They differ significantly from previous calculations. The effects of the different improvements are discussed.

Key words: atomic processes – diffusion – line: profiles – radiative transfer – stars: atmospheres – stars: chemically peculiar

1. Introduction

Photoabsorption processes produce radiative accelerations acting selectively on different atoms and ions in stellar atmospheres. This is now recognized (see the proceedings published by Michaud & Tutukov 1991, and Dworetsky et al. 1993) as the basic mechanism leading to the chemical peculiarities observed in main-sequence stars. Following the papers by Michaud (1970) and Michaud et al. (1976), quantitative models have been developed to explain the various observed abundances and their correlation with stellar characteristics: effective temperature ($T_{\rm eff}$), evolutionary stage, magnetic structure...

Theoretical investigations of particle transport depend mainly on the opposition between radiative acceleration and gravity and so pose the challenge to calculate precisely the radiative acceleration. A compromise between two opposite goals is needed: on the one hand the required accuracy (about 10%) implies the use of refined atomic physics (Michaud 1987,1993); on the other hand, the results should be obtained for an extensive number of atoms, ions and plasma conditions. In order to facilitate the astrophysical applications, Alecian & Artru (1990) have proposed an approximate expression for the radiative acceleration, using two parameters obtained from atomic and statistics physics. For example, this method is useful in order to introduce the radiative diffusion into stellar evolutionary codes (e.g. Richer & Michaud 1993). The accurate calibration of the fitted atomic parameters depends on the precision of the detailed calculations.

This paper describes the present state-of-the-art in detailed calculations of radiative accelerations, assuming Local Thermodynamical Equilibrium (LTE). A wide range of temperatures and densities which covers all radiative stellar envelopes and the deepest photospheric layers is considered. The results should not be used in stellar atmospheres since the diffusion approximation hypothesis is used for radiative transfer.

Our main purpose is to give a synthesis of the methods and approximations proposed in several previous theoretical papers and to point out the recent improvements which have become possible, thanks to the extended atomic database of the OPACITY project, subsequently referred to as OP (Seaton 1987; Seaton et al. 1992), which is now accessible to astrophysicists (Cunto et al. 1993a,b). In particular, we use the data for H, He, C, N, O, and Fe, the relevant calculations being described by

Send offprint requests to: M.-C. Artru (first address)

© European Southern Observatory • Provided by the NASA Astrophysics Data System

1995A&A...297..223G

Fernley et al. (1987), Peach et al. (1988), Luo & Pradhan (1989), Tully et al. (1990), and Butler et al. (1993).

We first summarize the basic definitions and the formalism leading to the radiative acceleration ($g_{\rm rad}$) on a given element. In subsequent sections, we detail the steps of the computation and our proposed improvements: the evaluation of the background continuum opacity, the refined approximations for line broadening, methods of distributing the acceleration between adjacent ions, and the addition of the radiative acceleration due to photoionization.

Examples of results are given throughout the paper in order to illustrate the successive improvements and to compare the different levels of approximation. They will concern either carbon or iron, in all their ionization stages; the radiative acceleration for these two elements of important astrophysical interest are under current investigation by the authors (Gonzalez et al. 1994; LeBlanc & Michaud 1994). Since the data for Fe I and Fe II is not included in OP, we will use the line data of Kurucz (1990,1991) for these ions. Their radiative acceleration and opacity due to photoionization are neglected since the corresponding data is not given by Kurucz.

To facilitate comparisons, we have chosen to display all the results for the same stellar envelope model having an effective temperature of 8000 K, a gravity $g = 10^{4.2}$ cm s^{-2}, with metallicity $Z = 0.02$ and relative metal solar abundances taken from Grevesse & Noels (1993). This stellar model was calculated as in Richer & Michaud (1993), but using the latest version of the OPAL opacities (Iglesias et al. 1992). We will also present each newly calculated radiative acceleration with reference to a basic standard approximation which is summarized as follows: the radiative acceleration is summed over the lines only (excluding the photoionization), the background absorption coefficient $\kappa_{\rm b}(\nu)$ (see Sect. 2) is given with the fitted formula of Borsenberger et al. (1979) (see Sect. 3), the coefficient of pressure broadening is the one given by Alecian & Artru (1990) (see Sect. 4), the radiative acceleration is summed for each ion, without distribution between adjacent ions, and the average over the different ions of charges Z_i is weighted by $\overline{Z}^2/Z_i^2$ (see Sect. 5).

2. Basic equations

The net momentum transported by a radiation flux $\mathscr{F}_\nu$ across the surface dS in time dt and frequency interval $d\nu$ is

$$dp_\nu\, d\nu = \frac{\mathscr{F}_\nu}{c}\, dS\, dt\, d\nu. \tag{1}$$

The differential radiative force pushing a particle of element A, with ionic charge i, undergoing the transition j (bound-bound or bound-free) with the cross-section $\sigma_{ij}(\nu)$, caused by photons with frequencies in the range $(\nu, \nu + d\nu)$ is then

$$F_\nu^{ij}\, d\nu = \frac{dp_\nu}{dt}\, d\nu = \sigma_{ij}(\nu)\, \frac{\mathscr{F}_\nu}{c}\, d\nu. \tag{2}$$

In stellar interiors (where $\tau_\nu \gg 1$), one can apply the diffusion approximation and assume LTE, which yields for the radiation flux

$$\mathscr{F}_\nu = -\frac{4\pi}{3}\, \frac{1}{\rho\kappa(\nu)}\, \frac{\partial B_\nu}{\partial T}\, \frac{dT}{dr}, \tag{3}$$

(see for example Eqs. 2-91 of Mihalas 1978) where $B_\nu(T)$ is the specific intensity of a black body of temperature T (Planck function) and

$$\kappa(\nu) = \frac{1}{\rho} \sum_n N_n \sigma_n(\nu) \tag{4}$$

is the total monochromatic opacity per unit mass at frequency ν, the sum of all absorption or scattering processes caused by the species present in the mixture (N_n is the number density of the initial state). In this paper, we note $\kappa_{\rm b}(\nu)$ the total opacity at frequency ν minus the contribution $\kappa_{ij}(\nu)$ of the transition being considered, and refer to it as the background opacity. The total opacity may then be written as

$$\kappa(\nu) = \kappa_{\rm b}(\nu) + \kappa_{ij}(\nu). \tag{5}$$

The reason for this definition of the total opacity is discussed in Sect. 3.

The temperature gradient can be derived from the assumption of radiative equilibrium and the definition of the Rosseland opacity $\bar{\kappa}_{\rm R}$:

$$\frac{dT}{dr} = -\frac{3}{16}\, \rho\, \bar{\kappa}_{\rm R}\, \frac{R^2}{r^2}\, \frac{T_{\rm eff}^4}{T^3}, \tag{6}$$

which gives the expression

$$F_\nu^{ij}\, d\nu = \frac{\pi k^4 T_{\rm eff}^4}{2h^3c^3}\, \frac{R^2}{r^2}\, \frac{\bar{\kappa}_{\rm R}}{\kappa_{\rm b}(\nu) + \kappa_{ij}(\nu)}\, \sigma_{ij}(\nu)\, P(u)\, du, \tag{7}$$

where

$$u = \frac{h\nu}{kT}, \tag{8}$$

$$P(u) = u^4\, \frac{e^u}{(e^u - 1)^2}, \tag{9}$$

R is the stellar radius, and r the distance from the center.

In the case of a bound-bound (b-b) transition, the cross-section is

$$\sigma_{ij}(\nu) = \frac{\pi e^2}{m_{\rm e} c}\, f_{ij}\, \phi_{ij}(\nu), \tag{10}$$

where f_{ij} is the oscillator strength of transition j, and the line absorption profile, $\phi_{ij}(\nu)$, is normalized to 1 (see Sect. 4).

For a bound-free (b-f) transition from ion A^i, the momentum of the incident photon is not transmitted entirely to ion A^{i+1}, but part of it is taken away by the ejected electron. One must then include a correction factor $f_{\rm ion}$, defined as the fraction of the momentum transferred to ion A^{i+1} (see Sect. 6).

© European Southern Observatory • Provided by the NASA Astrophysics Data System

1995A&A...297..223G

Integrating Eq. (7) over all frequencies and dividing by the mass m_A of element A, one obtains the contribution of transition j to the radiative acceleration on A^i:

$$\begin{cases} \text{b}-\text{b}: g_{\text{rad}}^{ij} = \dfrac{\pi k^4 T_{\text{eff}}^4}{2h^3c^3}\dfrac{R^2}{r^2}\dfrac{\bar{\kappa}_{\text{R}}}{X(A^i)}\times \\ \qquad \displaystyle\int_0^\infty \frac{\kappa_{ij}(\nu)}{\kappa_{\text{b}}(\nu)+\kappa_{ij}(\nu)}P(u)\,du \\ \text{b}-\text{f}: g_{\text{rad}}^{ij} = \dfrac{\pi k^4 T_{\text{eff}}^4}{2h^3c^3}\dfrac{R^2}{r^2}\dfrac{\bar{\kappa}_{\text{R}}}{X(A^i)}\times \\ \qquad \displaystyle\int_0^\infty \frac{\kappa_{i-1,j}(\nu) f_{\text{ion}}}{\kappa_{\text{b}}(\nu)+\kappa_{i-1,j}(\nu)}P(u)\,du, \end{cases} \tag{11}$$

where $X(A^i)$ is the massic abundance of ionization stage i. The total radiative acceleration on A^i is then

$$g_{\text{rad}}^i = \sum_{j,\text{b}-\text{b}} g_{\text{rad}}^{ij} + \sum_{j,\text{b}-\text{f}} g_{\text{rad}}^{ij} \tag{12}$$

In first approximation, one may consider that each ion diffuses through fully ionized hydrogen, with a diffusion coefficient D_i and a velocity v_i, given by a diffusion equation of the type

$$N_i v_i = D_i\left(-\frac{dN_i}{dr} + N_i\frac{m_A(g_{\text{rad}}^i - g)}{kT}\right), \tag{13}$$

where N_i is the number population of A^i. To simplify the present discussion, only the radiative and gravitational forces have been written in Eq. (13). The complete diffusion equation includes additional terms for thermal diffusion and electric fields, which do not directly affect radiative accelerations.

When many chemical elements diffuse relative to each other, the diffusion of an element modifies the diffusion of the others. An accurate determination of thermal diffusion and of the interaction terms requires solving a system of equations for heat fluxes, electric field and diffusion velocities of the various species (Burgers 1969). Once one uses such a system of equations coupling the diffusion of the various elements, it is nearly as simple to extend this system to include separately each state of ionization. The appropriate equations and constants are discussed in Michaud & Proffitt (1993).

Equation (13) is based on the assumption that D_i does not depend on the excitation state of A^i (see Sect. 5), and that an equilibrium balance exists between ionization and recombination. We neglect any coupling of ionization with diffusion; this may be important at lower densities, as discussed by Babel & Michaud (1991).

In order to describe the migration of element A through the stellar envelope, it is often convenient to write a single diffusion equation similar to Eq. (13), without subscripts i. The mean radiative acceleration g_{rad} entering this equation depends on the choice of the mean diffusion coefficient $\overline{D}$ adopted for element A. It may be defined as

$$\overline{D} = \frac{\sum_i N_i D_i}{\sum_i N_i} = \frac{\sum_i N_i D_i}{N}, \tag{14}$$

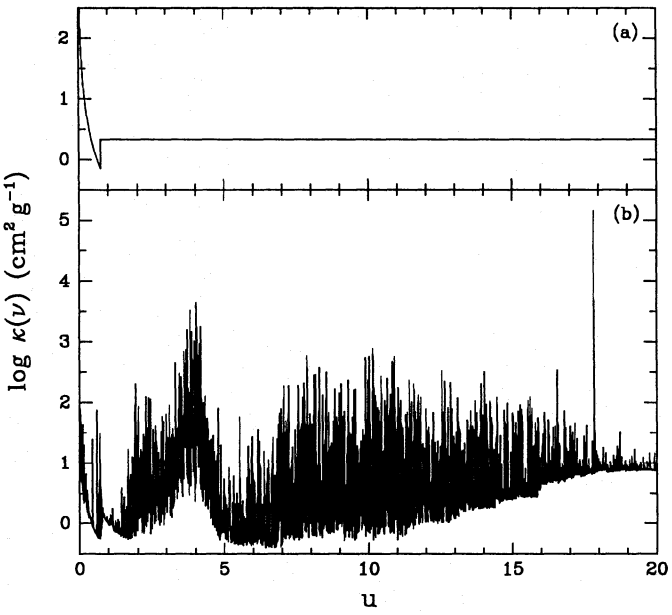

Fig. 1a and b. Opacity spectrum calculated in the same conditions as in Fig. 8b of Iglesias et al. (1992): $\log T = 5.3$ and $\log R = -5$, where $R = \rho/T_6^3$ is the parameter used by the OPAL group. **a** Average formula of Borsenberger et al. (1979). **b** Our calculation

and the radiative acceleration on element A is then

$$g_{\text{rad}} = \frac{\sum_i N_i D_i g_{\text{rad}}^i}{N\overline{D}} = \frac{\sum_i X(A^i) D_i g_{\text{rad}}^i}{X(A)\overline{D}}. \tag{15}$$

3. Opacity spectrum

As seen in Sect. 2, the total opacity at each frequency is needed to evaluate radiative accelerations. Previous studies (Alecian et al. 1993; Borsenberger et al. 1979,1981) used for the background opacity the simple formula proposed by Borsenberger et al. (1979, Eq. (8)). It was eye-averaged to an opacity spectrum calculated by Cox (1977) and scaled to the Rosseland mean opacity in order to be applicable in models using different opacity tables. The fitting formula has little monochromatic structure (see Fig. 1a) and is a source of uncertainty in radiative acceleration computations.

In order to improve the evaluation of the background opacity we have calculated monochromatic opacities at 4000 frequency points including the contributions of the elements listed in Table 1. These points are equally spaced and restricted to the $0 \le u \le 20$ domain. The opacities are computed on a grid with 21 values of R_{e}, within the range $-3.0 \le \log R_{\text{e}} \le 7.0$ where

$$R_{\text{e}} = N_{\text{e}}/T^3 \tag{16}$$

and for the same 50 temperature values used by the OPAL group (Rogers & Iglesias 1992). The parameter R_{e} is introduced by analogy to the one used in OPAL tables, but based on the electronic density instead of the mass density. We limited ourselves to those elements because of the size of the required data files.

© European Southern Observatory • Provided by the NASA Astrophysics Data System

1995A&A...297..223G

Table 1. Abundances used in the monochromatic opacity calculations

Element	Massic abundance
H	0.70000 = X
He	0.28000 = Y
C	0.00347
N	0.00106
O	0.00965
Fe	0.00155

The chosen composition of the plasma is given in Table 1. The four elements C, N, O, and Fe have solar relative abundances (Grevesse & Noels 1993), their absolute values are scaled to obtain $Z = 0.02$. The relative metal solar abundances used here are those presently used by the OPAL and OP groups. The major difference between these abundances and those of Anders & Grevesse (1989) is that the photospheric abundance of iron (Grevesse & Noels 1993) is closer to the meteoritic value since recent studies (e.g. Hannaford et al. 1992) favor this value.

Both the bound-bound and bound-free transitions given in the OP atomic database are included. Our frequency steps are large enough not to introduce the detailed profiles of the spectral lines except for the Lyman and Balmer lines of hydrogen. These series are computed with the parametrized profiles of Clausset et al. (1994). Thompson scattering is also included in our calculations. The atomic populations are calculated with the formalism of Hummer & Mihalas (1988), except for Fe I and Fe II which are treated classically. The partition functions used for these two ions are taken from the ATLAS code (Kurucz 1979).

An example of an opacity spectrum for our mixture is presented in Fig. 1b. This figure can be compared to Fig. 8b of Iglesias et al. (1992) and this shows that the opacities calculated here with the OP data are in good agreement with those of OPAL, even with the limited number of elements used. However, our opacities are undervalued by at least a factor of 4, as compared to OPAL, for photon energies for which $u \gtrsim 15$. In this energy range, the radiative acceleration is weakly affected because of the small value of $P(u)$, which gives the frequency dependence of the flux (Eq. (9)). It will also be interesting to compare our results to those of OP (Seaton et al. 1994) when their monochromatic opacities are available. Figure 1a shows the previously mentioned fitting formula which approximates the background monochromatic opacities. Comparing Figs. 1a and 1b shows that the approximate formula underestimates the opacity at most frequencies which usually causes an overestimate of radiative acceleration as will be seen below.

Since all metals are not included in our computations and since the fine structure is neglected, the Rosseland mean calculated with our monochromatic opacities, $\bar{\kappa}_R$, is expected to differ from the OP (Seaton et al. 1994) and OPAL (Iglesias et al. 1992) ones, $\bar{\kappa}_{OP}$ and $\bar{\kappa}_{OPAL}$. These three opacities are compared in Fig. 2, in the standard 8000 K, $\log g = 4.2$ stellar model calculated with OPAL opacities. $\bar{\kappa}_{OP}$ and $\bar{\kappa}_{OPAL}$ are very similar; a discussion of their discrepancies is given by Seaton et al. (1994). The Rosseland mean calculated in this paper is very close to those of OP and OPAL for $\log T < 4.8$ and is smaller by at most 0.5 dex for higher temperatures. The comparison of Fig. 2 to Fig. 9 of Seaton et al. (1994) indicates that the difference is mainly due to the contribution of elements heavier than Ne.

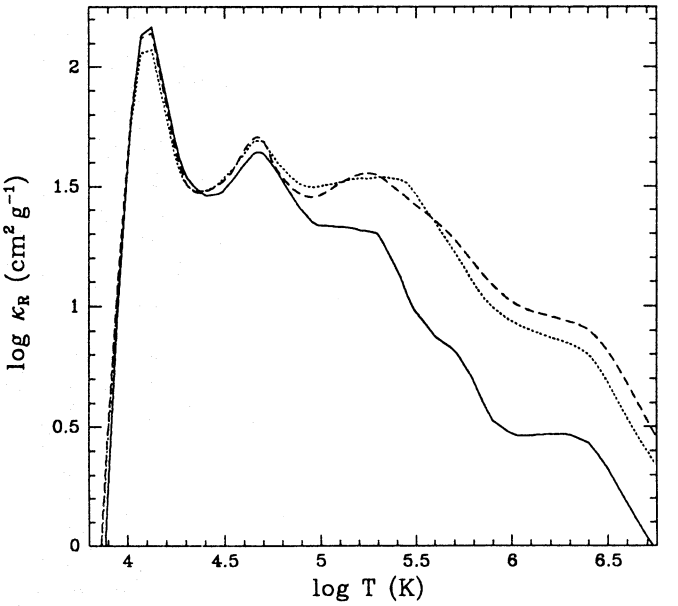

Fig. 2. Rosseland mean opacity calculated in this paper (solid line), that given by OP (dotted line) and by OPAL (dashed line) for our standard model with $T_{\rm eff}$ = 8000 K, $\log g = 4.2$ and $Z = 0.02$

Our limited mixture gives a reasonable estimate of the Rosseland mean. However, in the $g_{\rm rad}$ calculations, we prefer to use $\bar{\kappa}_{OPAL}$ instead of $\bar{\kappa}_R$ in the numerator of Eq. (11), since the former is more accurate and was used to construct the model. To maintain self-consistency, the monochromatic opacities appearing in the denominator of Eq. (11) were scaled by the factor $\bar{\kappa}_{OPAL}/\bar{\kappa}_R$. This scaling is especially critical in the deeper layers, where the monochromatic opacities calculated here are underestimates due to the missing elements. In the outer atmospheric layers, the Rosseland mean is too low since the opacity of H^- is not included.

It should be stressed that since the opacity spectrum is calculated for a limited number of frequency points, the rapid opacity changes inside line profiles are not resolved. In Eq. (11), the frequency variation of the opacity spectrum is included by defining a total opacity which equals the background opacity plus, separately, the opacity of the transition considered (see Eq. (5)). The background opacity is defined as the monochromatic opacity minus the contribution of the transition, in order not to include the contribution of this transition twice in the total opacity.

The difference in radiative accelerations computed with the monochromatic opacities calculated here and with the old fitting formula is shown in Fig. 3. The radiative acceleration of the bound-bound transitions is changed by less than 0.4 dex due to the inclusion of the frequency dependence of the background opacity. These results suggest that the previous approximation is reasonably accurate, at least in the upper layers of the envelope.

© European Southern Observatory • Provided by the NASA Astrophysics Data System

1995A&A...297..223G

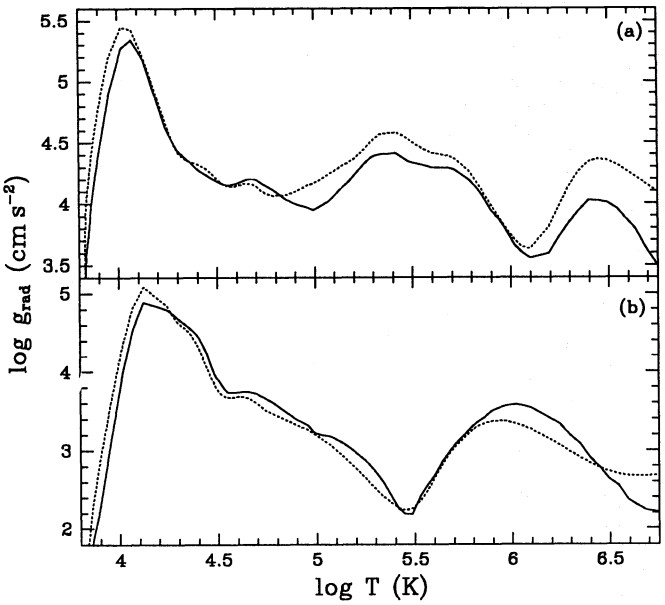

Fig. 3a and b. Radiative acceleration (b-b transitions) computed with the use of the formula of Borsenberger et al. (1979, reference calculation, dotted line) compared to the one calculated with the background opacity calculated in this paper (solid line): **a** for iron, **b** for carbon

4. Line profiles

In a stellar plasma, the line absoption profile $\phi_{ij}(\nu)$ is determined by several processes. First, the natural damping, referring to the finite lifetime of a level caused by its radiative decay, produces a Lorentz profile of full width at half-maximum (FWHM) $\Delta\nu_R$. Collisions with other particles of the plasma in addition induce pressure broadening, whose profile is also Lorentzian in the case of the quadratic Stark effect, of width $\Delta\nu_C$. Finally, each profile is Doppler-shifted according to the absorber's velocity on the line-of-sight; the corresponding velocity distribution being Maxwellian in LTE.

The resulting profile, i.e. the superposition of all the individual profiles, is then a convolution of a Gauss profile of width $\Delta\nu_D$ and of a Lorentz profile of width $\Delta\nu_R + \Delta\nu_C$:

$$\phi_{ij}(\nu) = \frac{1}{\sqrt{\pi}\,\Delta\nu_D} H(a, v), \tag{17}$$

where

$$a = \frac{\Delta\nu_R + \Delta\nu_C}{2\Delta\nu_D}, \tag{18}$$

and $H(a, v)$ is the Voigt function. Equation (17) ensures that $\phi_{ij}(\nu)$ is normalized to 1. It is important to use as accurate line widths as possible, since they determine the saturation and so the critical abundance for which $g_{rad} = g$.

The radiative width is given by

$$\Delta\nu_R = \frac{1}{2\pi}\left(\frac{1}{\tau_L} + \frac{1}{\tau_U}\right), \tag{19}$$

where τ_L and τ_U are the lifetimes of the lower and upper energy levels of the transition; and the Doppler width is

$$\Delta\nu_D = \frac{\nu_0}{c}\sqrt{\frac{2kT}{m_A}}, \tag{20}$$

ν_0 being the central frequency of the transition.

The evaluation of the pressure width requires a quantum mechanical approach, involving elaborate calculations for each line. An exact treatment is unrealistic in astrophysical problems where one has to take hundreds of thousands of lines. Previous radiative acceleration calculations (e.g. Alecian et al. 1993) used a semi-empirical approximation:

$$\Delta\nu_C = \gamma \frac{n_L^4 + n_U^4}{(Z_i + 1)^2} \frac{N_e}{\sqrt{T}}, \tag{21}$$

where n_L and n_U are the principal quantum numbers of the lower and upper levels, Z_i is the charge of the ion, and N_e is the electron density (see Griem 1960,1968 and Cox 1965). The numerical value of the coefficient γ can be taken from Griem (1968):

$$\gamma = \frac{5h^2}{3\pi m_e \sqrt{6\pi m_e k}}\,\bar{g} = 3.3\,10^{-6}, \tag{22}$$

if the Gaunt factor $\bar{g}$ is approximated to 0.2, and when $\Delta\nu_C$ is in s^{-1}, N_e in cm^{-3}, and T in K. This coefficient was subsequently calibrated with different experimental or more refined theoretical results and was taken equal to $1.6\,10^{-6}$ by Michaud et al. (1976, Eq. (32)), to both $1.6\,10^{-6}$ and $1.6\,10^{-5}$ by Michaud et al. (1983), to $2.0\,10^{-5}$ by Cox (1965), to $1.9\ 10^{-6}$ by Alecian & Michaud (1981, Eq. (2.6)), to $8.0\,10^{-6}$ by Alecian & Artru (1990, Eqs. (8) and (9)), and to $6.3\ 10^{-6}$ by Alecian et al. (1993, Eq. (1)). The calculation of g_{rad} used as reference takes the value $\gamma = 8.0\,10^{-6}$ given by Alecian & Artru (1990), which was calibrated with line widths obtained by the more elaborate modified semi-empirical (MSE) approximation described below.

For hydrogenic ions, the linear Stark effect is the dominant broadening process. To take it into account, we follow the approximation of Cox (1965) and raise the quantum numbers n_L and n_U to the fifth power instead of the fourth.

In order to improve the treatment of the collisional broadening, we used the MSE approximation developed by Dimitrijević & Konjević (1980,1986,1987). They gave the quadratic Stark width

$$\Delta\nu_C \propto \sum_{L'} |\langle L|r|L'\rangle|^2\,\bar{g} + \sum_{U'} |\langle U|r|U'\rangle|^2\,\bar{g}, \tag{23}$$

where the sums run over all levels perturbing the lower and upper levels of the transition being considered, using the hydrogenic approximation to obtain the matrix elements. It is now possible to have better values of $\Delta\nu_C$, since one has access to an extensive set of atomic data. The matrix elements for each perturbing transition $L \rightarrow L'$ or $U \rightarrow U'$ were then computed

© European Southern Observatory • Provided by the NASA Astrophysics Data System

1995A&A...297..223G

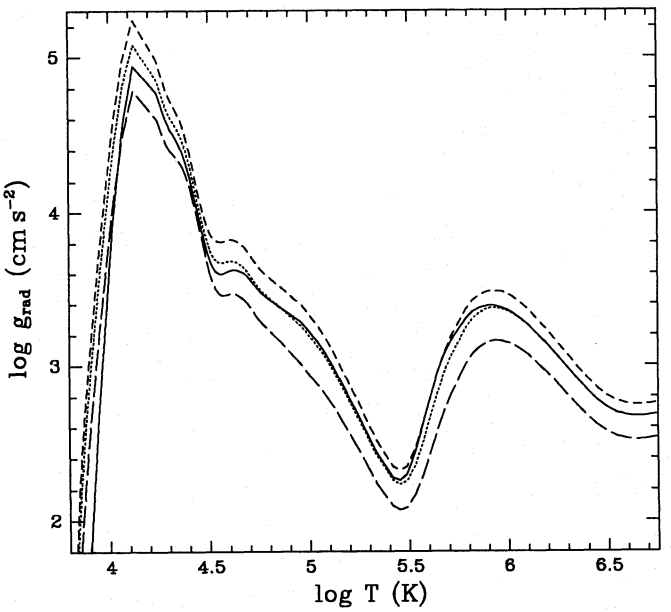

Fig. 4. Radiative acceleration of carbon (b-b transitions) computed using Eq. (21) for the pressure width, with $\gamma = 1.6\,10^{-6}$ (long dashes), $\gamma = 8.0\,10^{-6}$ (reference calculation, dotted line), and $\gamma = 2.0\,10^{-5}$ (short dashes) compared to the one using the MSE formula (solid line)

using the oscillator strengths provided in the OP database. The final expression for the Stark width is

$$\Delta\nu_c = \frac{2e^4}{3hc}\sqrt{\frac{6\pi}{m_e k}} \times \left[\sum_{L'} \lambda_{LL'} f_{LL'} \bar{g} + \sum_{U'} \lambda_{UU'} f_{UU'} \bar{g}\right] \frac{N_e}{\sqrt{T}}. \quad (24)$$

The Gaunt factors $\bar{g}$ are given in Appendix A, as well as the justification of Eq. (24). It must be pointed out, however, that this method is not valid for the linear Stark effect of H-like ions. We then kept for these ions the same pressure widths as in our reference calculation exposed above. Linear Stark profiles for H-like ions of CNO are being calculated by Stelhé (1994) and should be included in future studies.

The effect of using the MSE formula can be seen in Fig. 4, where the newly calculated g_{rad} for carbon is compared to the reference calculation. Are also shown on this figure radiative accelerations for which the pressure width was taken from Eq. (21) with the two extreme values of γ: $1.6\,10^{-6}$ and $2.0\,10^{-5}$. The last two examples differ by as much as 0.3 dex on average. The calculation using $\gamma = 8.0\,10^{-6}$ does not differ from the more exact MSE calculation by more than 0.1 dex, the agreement being better in the region $4.7 \leq \log T \leq 5.4$, where the ions whose widths were used for the calibration of γ (C III and C IV) are dominant.

5. Distribution of radiative acceleration among ions and averaging.

In a stellar plasma an element is usually in two or more states of ionization and a large number of excited levels are significantly occupied. In principle, each excited level of each state of ionization has its own collision cross-section and diffusion coefficient. For neutral states, the collision cross-sections may vary considerably from one excited level to the next since collisions between neutrals are influenced by the radius dependence of the electron distribution. For excited states of ionized elements, however, the collision cross-section depends on the coulomb field at large distances which essentially depends only on the net charge of the ion. The dependence of the diffusion coefficient on the state of excitation is considered by LeBlanc & Michaud (1993). In this paper only the dependence on the state of ionization is taken into account (see Appendix B).

The averaging of Eq. (15) depends first on the diffusion coefficients D_i of each ion A^i and on the choice of the adopted mean value $\overline{D}$. The average adopted here (see Eq. (15)) is simply weighted by the populations: it gives a reasonable evaluation if the gradient of density remains weak, which is usually the case in stellar interiors.

This approach allows to separate the solution of the transport equation from the solution of the rate equations for excitation, ionization and recombination occurring in the plasma. An exact solution would require treating together as many Boltzmann equations as existing atomic states for all the ions present in the plasma. This would be too demanding in the stellar context.

The basic formulae to evaluate diffusion coefficients needed for the radiative diffusion calculations are recalled in Appendix B. They were established in the theoretical frame of the elastic interaction between spherical particles in a dilute mixture (Burgers 1969; Chapman & Cowling 1970). A general result for a positive ion A^i is that the diffusion coefficient D_i decreases with increasing ionic charge, proportionally to Z_i^{-2}. The diffusion coefficients D_0 of neutral species are much larger; Michaud et al. (1979) have suggested to adopt the ratio $D_0/D_1 = 100$, as a first approximation based on a detailed comparison of the helium results (see Appendix B). This assumption is used to calculate the mean g_{rad} from Eq. (15), the neutral case being simply included with the formal value $Z_0 = 0.1$.

The total radiative acceleration on ion A^i appears in Eq. (11) as a simple addition of the photon momenta absorbed by all the bound-bound transitions of this ion and the bound-free transitions of ion A^{i-1}. This neglects possible effects of ionization or recombination inside the stellar plasma. Any absorbing species may change its state of ionization before it completely loses the momentum acquired in the photoabsorption. Therefore this momentum must be partially attributed to other ions.

After excitation by absorption of a photon, in the ground state, say, ion A^i is in an excited state. It has a finite probability to ionize (mainly by electronic collisions), before being scattered by 90° (mainly by collisions with protons) and so losing the effect of the momentum gained by photon absorption. Since the scattering probability depends on the ionic charge

© European Southern Observatory • Provided by the NASA Astrophysics Data System

1995A&A...297..223G

(proportionally to D_i^{-1}, or Z_i^2, see below), the effect of the absorbed photon is lost more rapidly if the element ionizes after absorption of a photon than if it returns to the initial state. This consequently modifies the effectiveness of the radiative acceleration and leads one to define an effective radiative acceleration, $g_{\rm eff}$, that depends not only on photon absorption but also on the various collision processes involved. An ideal calculation of $g_{\rm eff}$ requires determining in detail what happens to ion A^i for each final excitation state of each state of ionization. Various processes are involved, since ionization can occur by the absorption of another photon, by the successive absorption of many photons (in which case one should determine the probability of each of the processes at each stage), by a series of electronic excitations or by a combination of these processes. This amounts to calculations of a complexity comparable to non-LTE calculations and will not be attempted here. An approximate evaluation of the distribution of the momentum after absorption is instead proposed.

It involves defining a radiative acceleration for each state of ionization and a way to approximate the averaging of the contributions of all states of ionization. The radiative acceleration so couples the various states of ionization and limits the gain in accuracy achieved by calculating the particle transport with separate equations for each state of ionization. In order to make it possible to carry out stellar evolution calculations treating each state of ionization separately for particle transport (Eq. 13), or using one average equation when it is sufficient (Eq. 15), we determine radiative accelerations for both cases.

The distribution correction is of special importance for neutral species, because of two opposite effects: first diffusion in the neutral state may be dominant, even at high temperature where ionization is nearly complete, because the diffusion coefficient is much larger for neutral than for ionized atoms; but conversely, its efficiency is reduced by the distribution, because of its small scattering cross-section which may result in its being ionized before being scattered. This will be illustrated in examples below.

Montmerle & Michaud (1976) have described a general formalism for the calculation of the average radiative acceleration. A detailed application to the case of helium is given by Michaud et al. (1979). They have pointed out that the more efficient reactions between ions are those induced by electronic collisions. After undergoing transition j, ion A^i may either stay in its state of ionization before losing the acquired momentum or ionize and then lose its momentum in the state A^{i+1} (it is higly unlikely that it will ionize again, since it is in a low energy level, see Fig. 5). Recombination processes are generally unimportant compared to ionization (see Appendix C). This implies distributing between ions A^i and A^{i+1} the momentum gained in transition j. It is distributed in proportions r_{ij} and $1 - r_{ij}$, where

$$r_{ij} = \frac{\beta_{\rm coll}}{\beta_{\rm coll} + \beta_{\rm ion}}, \tag{25}$$

$\beta_{\rm ion}$ being the ionization rate and $\beta_{\rm coll}$ the rate to which ion A^i transmits its additional momentum to the surrounding protons. We then define an effective radiative acceleration $g_{\rm eff}$ by

$$\begin{cases} g_{\rm eff}^{ij} = r_{ij}\, g_{\rm rad}^{ij} \\ g_{\rm eff}^{i+1,j} = (1 - r_{ij})\, g_{\rm rad}^{ij}. \end{cases} \tag{26}$$

The radiative acceleration on A^i ($g_{\rm rad}^i$) is then obtained from Eq. (12), replacing $g_{\rm rad}^{ij}$ with $g_{\rm eff}^{ij}$, and the total radiative acceleration on element A is calculated using Eq. (15). The effective acceleration was defined differently in previous studies (Michaud et al. 1976 or Vauclair et al. 1979). Only the radiative acceleration is here included in $g_{\rm eff}$. For accurate calculations, it will be included in the complete diffusion equation.

The rate $\beta_{\rm coll}$ is inversely proportional to the diffusion coefficient:

$$\beta_{\rm coll} = \frac{kT}{m_A\, D_i}, \tag{27}$$

and its value can be estimated from the formulae given in Appendix B, neglecting any possible variation with excitation state.

The evaluation of $\beta_{\rm ion}$ should include direct ionization as well as possible cascading processes (ionization after successive excitations and decays) and it strongly depends on the excitation state after photoabsorption. Appendix C recalls general formulae useful to calculate the different rates of excitation, de-excitation, ionization and recombination, induced either by the radiation field $B_\nu(T)$ or by electronic collisions. In principle this should allow to generalize the results obtained by Michaud et al. (1979) who treated the case of helium in detail.

For complex atomic structures, we suggest the use of a simplified model which consists in fixing a boundary according to the probability of excited states to ionize. For example the different rates are shown in Fig. 5 for several states of C^+ at the depth of our stellar model where this ion is dominant. We have selected the state which is the more often reached by b-b transitions for each value of the principal quantum number n of the outer electron. The excitation and de-excitation rates plotted here are summed over the transitions with $\Delta n \neq 0$. From this comparison it can be confirmed that direct radiative ionizations as well as both radiative and collisional recombination probabilities, are negligible. For all states with $n \geq 3$, the more rapid changes occurring after a photoabsorption are excitation and de-excitation with rates larger than $\beta_{\rm coll}$ by factors of 100 and more. This ensures that the relaxation time between the different excitation states is short compared to the scattering collision time scale $\tau_{\rm coll} = 1/\beta_{\rm coll}$ with protons. Direct ionization appears more probable than proton collisions for all excited states with $n \geq 4$. For $n = 3$, the ion will rapidly be excited to an upper state for which $\beta_{\rm ion} > \beta_{\rm coll}$. Once ionized into C^{2+}, it is in a low energy level; it is then very unlikely that it will either recombine into C^+, or ionize again before losing its momentum (the rates for $n = 2$ levels of C^{2+} have relative values comparable to those of C^+ shown in Fig. 5). Therefore, for all these rapidly ionized

© European Southern Observatory • Provided by the NASA Astrophysics Data System

1995A&A...297..223G

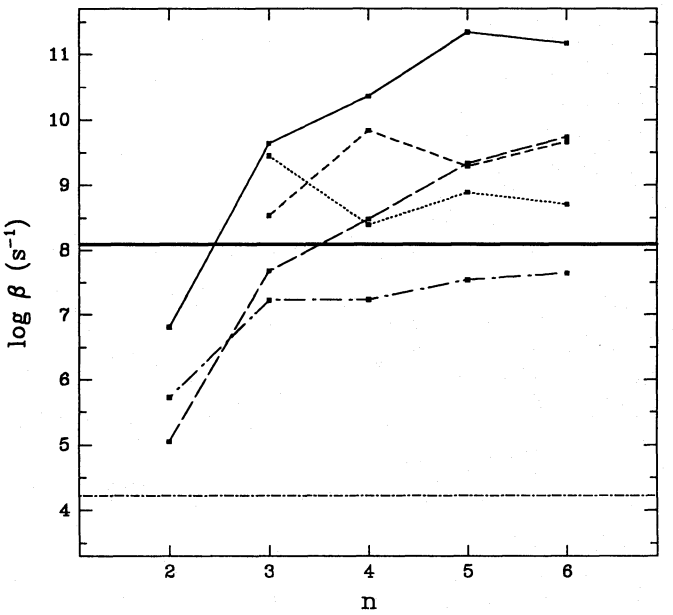

Fig. 5. Collisional excitation rate (solid line), collisonal de-excitation rate (short dashes), radiative de-excitation rate (dotted line), collisional ionization rate (long dashes), radiative ionization rate (dots-long dashes), and recombination rate (dots-short dashes) compared to $\beta_{\rm coll}$ (heavy solid line) for selected levels of C^+ (see text), at $T = 3.1\ 10^4$ K and $N_e = 1.6\ 10^{16}$ cm^{-3}; n is the quantum number of the outer electron

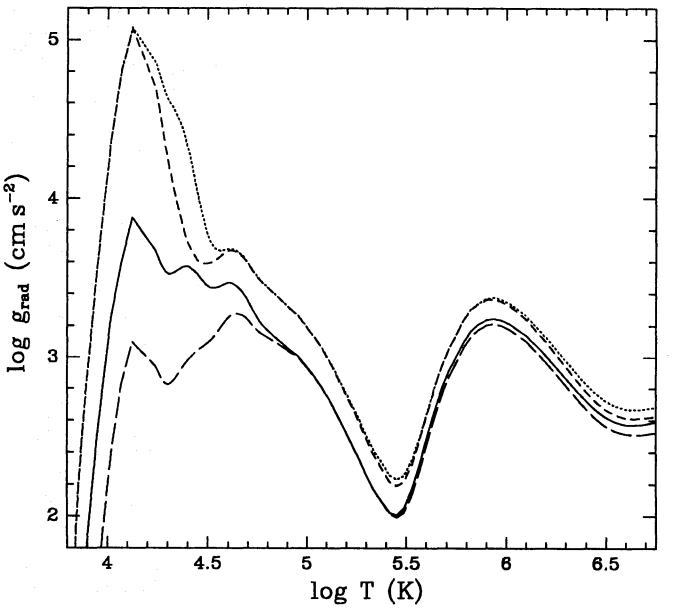

Fig. 6. Radiative accelerations for carbon (b-b transitions) computed without distribution (reference calculation, dotted line), with the distribution model proposed by Montmerle & Michaud (1976, short dashes), with our distribution model (solid line), and in the limit where $g_{\rm rad}^{ij}$ is entirely distributed to ion A^{i+1} for all transitions (long dashes)

states, we set $r_{ij} = 0$, while we take $r_{ij} = 1$ for the lowest states belonging to a configuration having a maximum value of $n = 2$, since even their excitation rate is smaller than $\beta_{\rm coll}$. From other comparisons (not shown), this model appears applicable to the different ions of C, N and O. For iron we will also use a model in which we set $r_{ij} = 1$ for the transitions ending in a state for which the principal quantum number is greater than that of the fundamental plus one. For the radiative acceleration due to photoionization, we will suppose that all of the momentum tranfered to the atom is spent in the newly ionized state.

In Fig. 6 is shown the radiative acceleration due to b-b transitions obtained for carbon using different options for redistribution. The correction of Montmerle & Michaud (1976) has little effect except in the region where $g_{\rm rad}$ is dominated by the contribution of the neutral state ($\log T < 4.5$). This can be explained by the fact that they only used the radiative ionization to compute $\beta_{\rm ion}$ and that the neutral atom, whose $\beta_{\rm coll}$ is smaller, may be the only ionization state for which radiative ionization dominates. The radiative acceleration calculated with our correction is reduced by 0.2 dex with respect to the reference calculation, and, as expected, the effect is greater for the neutral state, where the difference can reach 1.2 dex. The lower curve shows the radiative acceleration computed in the limit where ionization is dominant for all states, that is $r_{ij} = 0$ for all transitions.

6. Radiative acceleration due to photoionization

Since the OP atomic database contains photoionization cross-sections for all levels, it is now possible to study the importance of photoionization on the radiative force. In the past, the contribution of photoionization to the radiative accelerations could only be evaluated in the hydrogenic approximation (e.g. Michaud 1970).

As discussed briefly in Sect. 2, during photoionization, only part of the momentum of the photon is transferred to the ion. The factor $f_{\rm ion}$ introduced in Eq. (11) is needed for every energy level in order to properly calculate radiative acceleration due to photoionization. The only known quantum calculation of this correction factor is for the hydrogen fundamental state (Sommerfeld 1939). The correction factor in that case is

$$f_{\rm ion} = 1 - \frac{8}{5}\frac{h\nu - \chi}{h\nu}, \qquad (28)$$

where ν is the frequency of the ionizing photon and χ the ionization energy threshold. Calculations of $f_{\rm ion}$ for any nl orbital in a central potential are in progress (Massacrier 1994). The values of $f_{\rm ion}$ are also needed for complex ions. They cannot be computed from OP data; moreover, their extensive calculation would have been more lengthy than those performed by OP.

In this paper, we use the correction factor given above for all the energy levels of the elements studied. Examples of the possible importance of $f_{\rm ion}$ are given in Fig. 7. By adding the correction factor, the radiative acceleration due to photoionization can be diminished by as much as 0.9 dex for carbon and up to 0.4 dex for iron.

Alecian (1994) developed a method of approximation for the radiative acceleration due to photoionization, but as he mentioned, his method is not valid for abundant elements like CNO or Fe.

© European Southern Observatory • Provided by the NASA Astrophysics Data System

1995A&A...297..223G

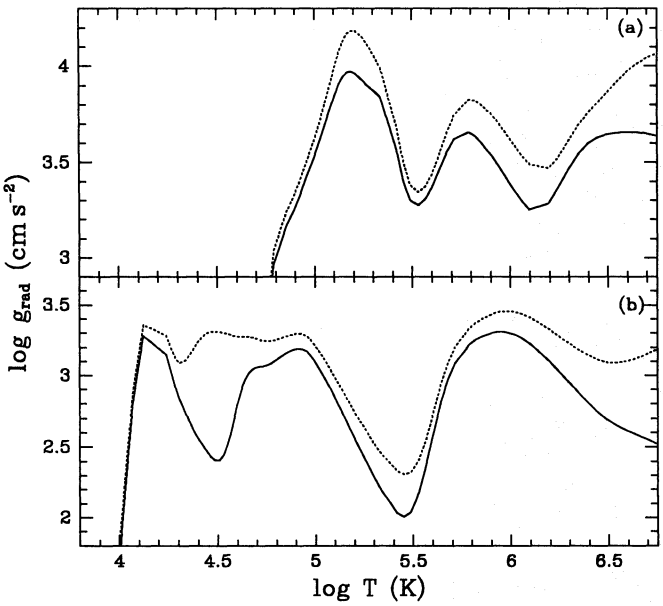

Fig. 7a and b. Radiative acceleration due to photoionization computed with $f_{ion} = 1$ (dotted line) compared to the one calculated with f_{ion} given in Eq. (28) (solid line): **a** for iron, **b** for carbon. The monochromatic opacity is that of Borsenberger et al. (1979) in both cases

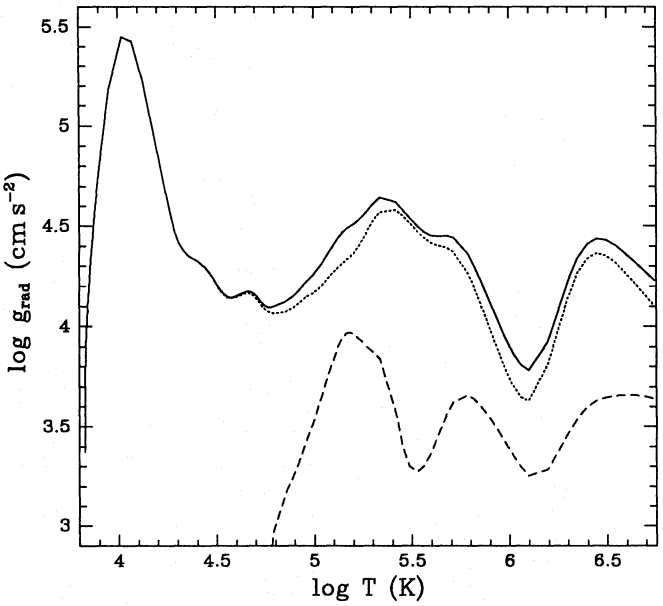

Fig. 8. Total radiative acceleration for iron (solid line) together with the contributions of b-b transitions (reference calculation, dotted lines) and of b-f transitions (with f_{ion} from Eq. (28), dashed line)

Examples of the relative importance of both b-b and b-f transitions are given for iron in Fig. 8. The radiative acceleration is increased by a maximum of 0.2 dex when photoionization is included.

7. Discussion

This paper puts together, from the many papers that have been published pertaining to radiative acceleration calculations, the various processes that need to be included to obtain accurate radiative accelerations. Emphasis has been put on the improvements made possible by using the atomic databases that have become available recently and on approximations that need improving.

For abundant ions, the broadening mechanism plays an important role in determining the radiative acceleration. A systematic use of semi-empirical approximations is proposed for the quadratic Stark broadening (Sect. 4) using the OP data. The broadening is specially critical for hydrogenic ions where the linear Stark effect is dominant. New calculations are currently underway for these ions (Stelhé 1994). They should be used in future work.

It has been shown how electronic excitation, electronic ionization, atomic scattering and photo-absorption cross-sections all play an important role in the distribution of the momentum absorbed from the radiation field among the various ionization states of the absorbing atomic species (Sect. 5). A simple model, based on a comparison of collision rates for the important processes, has been derived and shown to lead to reasonably accurate radiative accelerations for most cases. A more exact evaluation would require very elaborate calculations of the successive excitations and de-excitations following all photon absorptions.

The photoionization cross-sections calculated in the OP have made it possible to include the contribution of the bound-free transitions to the radiative acceleration calculations (Sect. 6). These however also require an evaluation of the fraction of the photon momentum given to the electron after ionization, demanding further calculations since it is currently available only for the ground state of hydrogenic ions.

Accurate radiative acceleration calculations consequently require determining not only how many photons are absorbed by each atomic element but also the state each ion is in after the absorption as well as the process causing the absorption since the distribution of the momentum among the ionization states is important and since special corrections must be applied after some processes, such as photoionization. The OP data base contains most of the needed information, except those necessary to calculate f_{ion}.

In the calculations of radiative accelerations done up to now it has been assumed that the continuum spectrum had a relatively simple form (see Sect. 3). This caused significant uncertainties in the radiative acceleration calculations, since the opacity at the frequency of absorption determines the fraction of the photons of that frequency absorbed by an ion (see Eq. (7)). It is now possible to calculate the opacity as a function of frequency using the OP data and use these for the radiative acceleration calculations (see Sect. 3). This was done here assuming that the main contributions to the opacity came from H, He, C, N, O and Fe. This led to the construction of a large table containing separately the contribution of H, He, C, N, O and Fe at each of 4000 frequency values, at each of 21 densities and at each of 50 temperature values. Although the total of some 50

© European Southern Observatory • Provided by the NASA Astrophysics Data System

1995A&A...297..223G

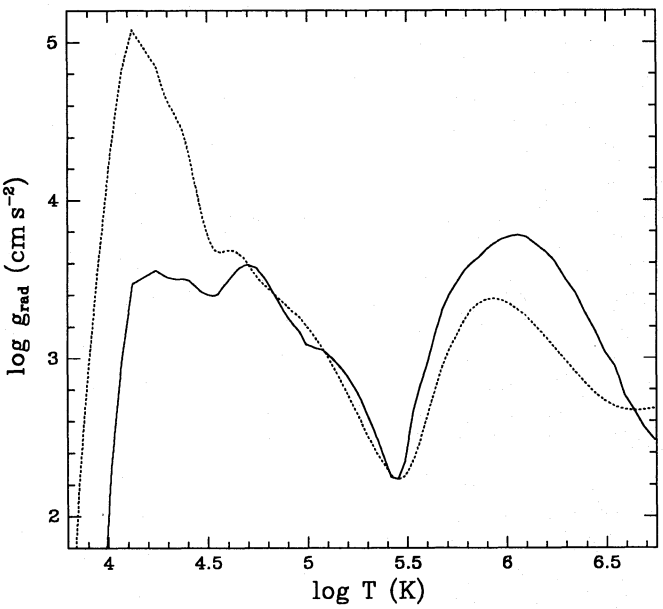

Fig. 9. Radiative acceleration for carbon. The reference calculation (dotted line) is compared to the calculation including all corrections mentioned in Sects. 3 to 6 (solid line)

Megabytes of data per element is large, it can be handled by modern computers. It is being used to calculate radiative acceleration calculations as a function of abundances for C, N, O and Fe which will be published separately (Gonzalez et al. 1994; LeBlanc & Michaud 1994). It would of course be preferable to include more atomic species in the continuum opacity calculations but the size of the data files required would become prohibitive for applications.

An example of the effect of all the corrections mentioned above is shown on Fig. 9 for carbon (solid line). The dotted line gives the reference calculation. Additional calculations of linear Stark broadening (Stehlé 1994) and of $f_{\rm ion}$ (Massacrier 1994) are underway and are not included. The difference between the reference calculations and the new ones is large at $T \sim 10^6$ K, where there is a potential effect of linear Stark broadening since C VI dominates, but it is mainly due to the inclusion of photoionization (see also Fig 7b) for which the ongoing calculations for $f_{\rm ion}$ could be important. The change in continuum opacity also plays a role (see Fig. 3b). The other large difference occurs at low temperatures. There it is related to the redistribution of the momentum absorbed by C I, since it has been found that ionization by successive collisions reduces the radiative acceleration considerably, although there remains some uncertainty in this correction factor. However, diffusion occurs only below the convection zone, that is for $\log T > 4.3$ in our standard model, where the latter effect is smaller. It is still important, though, at the bottom of the convection zone.

The availability of the radiative accelerations on the main contributors to the opacity (H, He, C, N, O and Fe) and of the tables containing their contribution to the opacity as a function of frequency makes it possible to calculate for the first time stellar evolution models containing all aspects of atomic diffusion. This requires calculating at the same time as stellar evolution, the particle transport of He, C, N, O and Fe using their radiative accelerations and recalculating continuously the Rosseland opacity for the mixture, taking into account the changes in abundance of He, C, N, O and Fe. However, detailed calculations of radiative accelerations for each layer, at each step of evolution would be too time consuming. The use of faster methods is then necessary: one can use either approximate formulae, such as that developed by Alecian & Artru (1990), calibrated according to the detailed calculations, or tables of radiative accelerations convenient for interpolation at the temperature, electronic density, and abundance of interest. The combination of such methods with the 50 Megabytes opacity tables mentioned above then allows a simultaneous calculation of evolution and diffusion. The contributions of over and underabundance to the background opacity can be taken into account in detail since the contribution to opacity is stored independently for each of H, He, C, N, O and Fe at each frequency for all densities and temperatures of interest.

Such stellar evolution calculations may then serve as reference showing the effect of unhampered atomic diffusion on stellar structure. They may be compared to the observations of AmFm stars as well as those of the Li gap stars in order to determine the extent of the effect of potential competing hydrodynamical processes (turbulence, meridional circulation, mass loss) on stellar structure.

One limitation of these calculations is that blends are not taken into account except in some average way (they are included in each of the 4000 frequency bins but they are spread over the bin). Blends could be important for some unabundant elements that would compete for photons with a strong line of an abundant element. Taking this into account requires the precise determination of the position of each line. This line position is not accurate enough in the OP database. Experimental wavelengths are used by Kurucz but his database covers only a fraction of the envelope that is of interest for stellar evolution calculations.

Finally, from the results of the radiative acceleration calculations presented here, it is already evident that at least Fe can be supported in parts of the envelope and so lead to overabundances, as already found by Alecian et al. (1993). This can modify the structure of those stars. It could even possibly lead to pulsations. This will be considered separately (Turcotte et al. 1994). The contribution of photoionization is never dominant for radiative accelerations. It is however large enough that it should not be neglected. It could lead to factors of about 1.5 in the equilibrium abundances of Fe at some places in stellar envelopes. Consequently it appears that all the processes considered here should be included in radiative acceleration calculations.

Acknowledgements. This research benefited from a financial support of the Centre Jacques Cartier and of NSERC. The authors would like to thank R. L. Kurucz for providing his atomic data and J. Richer for calculating the stellar envelope model used and for helpful discussions.

© European Southern Observatory • Provided by the NASA Astrophysics Data System

1995A&A...297..223G

Appendix A: quadratic Stark widths – MSE approximation

A.1. Neutral atoms

The half Stark width at half-maximum of level L, in angular frequency units, is given by Dimitrijević & Konjević (1986):

$$\frac{\Delta\omega_{\rm neutral}}{2} = \sqrt{\frac{32}{27}}\, N_{\rm e}\pi\, \frac{\hbar a_0}{m_{\rm e}} \sqrt{\frac{E_{\rm H}}{kT}} \times \sum_{L'} R^2_{LL'}\, f_w\!\left(\frac{R_{LL'}\,\Delta E_{LL'}}{3kT}\right), \quad \text{(A1)}$$

where the sum runs over all levels L' perturbing level L, $\Delta E_{LL'}$ is the energy difference between levels L and L', and

$$R^2_{LL'} = \frac{|<L|r|L'>|^2}{a_0^2}, \quad \text{(A2)}$$

and with

$$f_w(u) = e^{-1.33u}\,\ln\!\left(1+\frac{2.27}{u}\right) + \frac{0.487u}{0.153+u^{5/3}} + \frac{u}{7.93+u^3}. \quad \text{(A3)}$$

Using the expression of the Bohr radius $a_0 = \hbar^2/m_e e^2$ and of the Rydberg $E_{\rm H} = m_e e^4/2\hbar^2$, one gets, for the FWHM in frequency units:

$$\Delta\nu_{\rm neutral} = \frac{h^2}{3\pi^2 m_{\rm e} e\sqrt{3m_{\rm e}k}} \times \left[\sum_{L'} R^2_{LL'}\, f_w\!\left(\frac{R_{LL'}\,\Delta E_{LL'}}{3kT}\right)\right] \frac{N_{\rm e}}{\sqrt{T}}. \quad \text{(A4)}$$

A.2. Ions

Dimitrijević & Konjević (1987) give the full Stark width at half-maximum of level L, in angular frequency units:

$$\Delta\omega_{\rm ion} = N_{\rm e}\frac{8\pi}{3}\frac{\hbar^2}{m_{\rm e}^2}\sqrt{\frac{2m_{\rm e}}{\pi kT}}\,\frac{\pi}{\sqrt{3}}\sum_{L'} R^2_{LL'}\,\bar{g}\!\left(\frac{3kT}{2\Delta E_{LL'}}\right), \quad \text{(A5)}$$

where $\bar{g}$ is the Gaunt factor. They take the values of $\bar{g}(x)$ given by Griem (1968) in the case of transitions with $\Delta n \neq 0$. For transitions with $\Delta n = 0$, they refine the approximation, using the modified factor

$$\tilde{g}(x) = 0.7 - \frac{1.1}{Z+1} + \bar{g}(x) \quad \text{(A6)}$$

(Dimitrijević & Konjević 1980). When the energy of the perturbing electrons ($\frac{1}{2}mv^2 = \frac{3}{2}kT$) becomes large with respect to the energy difference $\Delta E_{LL'}$, the Gaunt factor must tend towards the quasi-classical GBKO result (Griem et al. 1962) given by Dimitrijević & Konjević (1980) in the form:

$$\bar{g}(x) = \tilde{g}(x) = \frac{\sqrt{3}}{\pi}\left(\frac{1}{2} + \ln\frac{4x(Z+1)}{3n_L^2}\right). \quad \text{(A7)}$$

The FWHM in frequency units can be written:

$$\Delta\nu_{\rm ion} = \frac{2h^2}{3\pi m_{\rm e}\sqrt{6\pi m_{\rm e}k}} \times \left[\sum_{L'} R^2_{LL'}\,\bar{g}\!\left(\frac{3kT}{2\Delta E_{LL'}}\right)\right] \frac{N_{\rm e}}{\sqrt{T}}. \quad \text{(A8)}$$

A.3. General formula

Equations (A4) and (A8) can be written in the general form:

$$\Delta\nu = \frac{2h^2}{3\pi m_{\rm e}\sqrt{6\pi m_{\rm e}k}}\left[\sum_{L'} R^2_{LL'}\,\bar{g}\right]\frac{N_{\rm e}}{\sqrt{T}}, \quad \text{(A9)}$$

defining

$$\begin{cases} \bar{g}_{\rm neutral} = \dfrac{1}{\sqrt{2\pi}}\, f_w\!\left(\dfrac{R_{LL'}}{2x}\right) \\ \bar{g}_{\rm ion} = \bar{g}(x). \end{cases} \quad \text{with } x = \frac{3kT}{2\Delta E_{LL'}}. \quad \text{(A10)}$$

The value $R^2_{LL'}$ can be calculated from the oscillator strength $f_{LL'}$ of transition $L \rightarrow L'$ at wavelength $\lambda_{LL'}$ (see e.g. Cowan 1981):

$$R^2_{LL'} = \frac{6\pi^2 m_{\rm e} e^4}{h^3 c}\lambda_{LL'} f_{LL'}, \quad \text{(A11)}$$

which gives:

$$\Delta\nu = \frac{2e^4}{3hc}\sqrt{\frac{6\pi}{m_{\rm e}k}}\left[\sum_{L'}\lambda_{LL'} f_{LL'}\,\bar{g}\right]\frac{N_{\rm e}}{\sqrt{T}}. \quad \text{(A12)}$$

The Stark width of a spectral line $L \rightarrow U$ is therefore

$$\Delta\nu_{\rm c} = \frac{2e^4}{3hc}\sqrt{\frac{6\pi}{m_{\rm e}k}} \times \left[\sum_{L'}\lambda_{LL'} f_{LL'}\,\bar{g} + \sum_{U'}\lambda_{UU'} f_{UU'}\,\bar{g}\right]\frac{N_{\rm e}}{\sqrt{T}}. \quad \text{(A13)}$$

Appendix B: diffusion coefficients

The diffusion coefficient D_i of ion A^i is defined by the diffusion equation (Eq. (13)). Basic formulae giving D_i are established in the theoretical frame developed in particular for spherical particles in a dilute mixture by Chapman & Cowling (1970).

B.1. Ions

In the case of ions, the dominant interaction is usually the long-range Coulomb force with protons. Equations (4-12) of Spitzer (1968) leads to

$$D_i = \frac{3\,k^2}{8\,e^4\,Z_i^2}\sqrt{\frac{2\,k}{\pi\,m_{\rm p}}}\sqrt{\frac{A+1}{A}}\,\frac{T^{5/2}}{N_{\rm e}}\,\frac{1}{\ln\Lambda}. \quad \text{(B1)}$$

© European Southern Observatory • Provided by the NASA Astrophysics Data System

1995A&A...297..223G

The proton mass and charge are noted m_p and e, those of the considered ion being $m_A = A\,m_p$ and $Z_i\,e$. The Coulomb logarithm $\ln\Lambda$ introduces the Debye screening limit in the effective range of the ion-proton interaction. It is given by the Spitzer (1968, Eq. (4-13)) formula:

$$\Lambda_{\rm Spitzer} = \frac{3\,k}{2\,e^3\,Z_i}\sqrt{\frac{k}{\pi}}\frac{T^{3/2}}{\sqrt{N_e}}. \qquad \text{(B2)}$$

To avoid divergence and negative logarithm for increasing Z_i and density, the cut-off value of $\ln\Lambda = 0.5$ is adopted at the limit of validity of the model (see e.g. Hansen 1980), so that

$$\ln\Lambda = \max(\ln\Lambda_{\rm Spitzer}, 0.5). \qquad \text{(B3)}$$

This gives a first approximation which is sometimes sufficient. More accurate values require replacing Coulomb potentials by Debye shielded potentials (Paquette et al. 1986) to calculate diffusion coefficients for the Chapman & Cowling (1970) or Burgers (1969) formalisms (Michaud & Proffitt 1993).

B.2. Neutral atoms

When the diffusing particle is neutral the interaction with protons is weaker and it depends on the atomic quantum state through its polarisability and the radius of its repulsive core.

We recall here the general formulae derived from the theoretical procedure detailed by Chapman & Cowling (1970, pp. 163-171).

In the model of hard-sphere collision (HS), the diffusion coefficient is obtained from Eqs (9.81,1) and (10.22,2) of Chapman & Cowling (1970) as a function of an effective core radius of the atom, $r_{\rm core}$:

$$D_0^{\rm HS} = \frac{3}{8}\sqrt{\frac{k}{2\pi\,m_p}}\sqrt{\frac{A+1}{A}}\frac{\sqrt{T}}{N_e}\frac{1}{r_{\rm core}^2}. \qquad \text{(B4)}$$

When the interaction is due to the atomic polarisability α, the interaction force is proportional to r^{-5}, leading to the formula (from Eqs (9.81,1) and (10.31,11) of Chapman & Cowling 1970):

$$D_0^{\rm pol} = \frac{k}{2\pi\,e\,A_1(5)\sqrt{2\,m_p}}\sqrt{\frac{A+1}{A}}\frac{T}{N_e}\frac{1}{\sqrt{\alpha}}, \qquad \text{(B5)}$$

where the value of $A_1(5) = 0.8$ for a repulsive force is given by Ratel (1975).

Examples of quantitative evaluation are given by Michaud et al. (1978) for the case of helium. They also applied a more realistic composite potential including the two previous effects, that is a short-range repulsion and a long-range attraction. They found that the HS approximation overestimates the diffusion coefficient (by a factor of about 5) and that the polarisation model gives a better estimate.

Equations (B4) and (B5) require the knowledge of the atomic core radius and of the polarisability. These atomic data may be found in different compilations such as Radzig & Smirnov (1985).

Table 2. Ratios D_0/D_1 for different atoms. The plasma conditions are defined by $\log R_e = 2.7$ and T such as $kT = I_0/10$

Element	I_0 (eV)	α (Å^3)	D_0/D_1
He	24.59	0.21	97
C	11.26	1.75	108
N	14.53	1.11	93
O	13.62	0.80	120
Na	5.14	24	95
Mg	7.65	11	77
Si	8.15	5.5	99
Ca	6.11	25	72
Fe	7.87	13	68

The ratio of diffusion coefficients between a neutral atom and the corresponding first ion is given by the ratio of Eqs. (B1) and (B5) as

$$\frac{D_0^{\rm pol}}{D_1} = 3.38\,10^{-5}\,\frac{\ln\Lambda}{\sqrt{\alpha\,T^3}}. \qquad \text{(B6)}$$

We have evaluated this ratio in typical stellar enveloppe conditions with $R_e = 2.7$ (see Eq. (16) for definition) for different elements. The temperature is chosen so that the contribution of the neutral to the radiative acceleration is dominant: this implies that kT is of the same order of magnitude as one tenth of the ionization energy of the atom I_0. Using the values of I_0 and α compiled by Radzig & Smirnov (1985), we found that $\sqrt{\alpha T^3}$ varies within a factor of 1.7 only. This leads to a mean value $D_0/D_1 \simeq 92$ (see Table 2), very similar to the value $D_0/D_1 = 100$ adopted in our calculation.

Appendix C: radiative and collisional rates

This appendix summarizes usual approximate formulae which allow to evaluate the different ionization and excitation rates. They are needed to calculate what happens to an ion after a photoabsorption, and to evaluate the distribution of the radiative acceleration, as shown in Sect. 5.

The rates β are defined as the probability per unit time of the reaction per ion. The functions are written using the fundamental constants, to help the comparison with other forms of similar approximations, given in textbooks, such as Jefferies (1968), Sobelman et al. (1981), or Mihalas (1978). Major simplifications of the theoretical results arise from the hypothesis that the reactions are mainly induced by photons of energies $h\nu$ much larger that kT and by weak inelastic collisions with thermal electrons.

C.1. Radiative processes

The radiative ionization rate used here is given by

$$\beta_{\rm ion,rad} = \frac{8\pi k^3}{c^2h^3}\,T^3\,\sigma_0\,u_0^2\,e^{-u_0}, \qquad \text{(C1)}$$

where the integration over frequencies has been performed with an hydrogenic variation law for the photoionization cross-sections, $\sigma = \sigma_0\,(u_0/u)^3$, assuming that thresholds satisfy

© European Southern Observatory • Provided by the NASA Astrophysics Data System

1995A&A...297..223G

$u_0 = h\nu_0/kT \gg 1$. This formula is commonly applied with the hydrogenic approximation for the threshold cross-section σ_0. Here we have instead introduced the values of σ_0 taken from the OP data.

The radiative rates for excitation and de-excitation can be directly derived from the gf values of the OP database. In our plasma conditions, only the spontaneous radiative decay may change the atomic state, the induced processes being less frequent by a factor of the order of $\exp(-h\nu/kT)$.

C.2. Collisional processes

To evaluate the electronic collisional rates, we use the ratio between corresponding radiative and collisional cross-sections (it is then limited to allowed transitions) as described by Seaton (1962). This ratio is approximated by means of the empirical average Gaunt factor $\bar{g}$ that has already been introduced for line broadening (Sect. 4 and Appendix A).

The formulae giving collisional de-excitation and excitation rates from level L to level L', consistent with detailed balance, may be written:

$$\beta_{\mathrm{ex,coll}} = \frac{4\pi e^4}{k}\sqrt{\frac{2\pi}{3m_e k}}\frac{N_e}{T^{3/2}} f_{LL'}\bar{g}\frac{e^{-u}}{u} \qquad \text{(C2)}$$

$$\beta_{\mathrm{de-ex,coll}} = \frac{4\pi e^4}{k}\sqrt{\frac{2\pi}{3m_e k}}\frac{N_e}{T^{3/2}} f_{LL'}\bar{g}\frac{1}{u} \qquad \text{(C3)}$$

The expression of the ionization rate is derived from the radiative ionization rate (Eq. (C1)):

$$\beta_{\mathrm{ion,coll}} = \frac{4e^2c}{h}\sqrt{\frac{2\pi m_e}{3k}}\frac{N_e}{\sqrt{T}}\sigma_0\bar{g}\frac{e^{-u_0}}{u_0} \qquad \text{(C4)}$$

It is equivalent of the one given by Mihalas (1978, p. 134), the numerical value of the constant coefficient being $1.55\ 10^{13}$ (cgs-esu).

The recombination rate for ion A^{i+1} should include all the ways of recombination towards all possible states of ion A^i. Therefore the total result cannot be expressed in a simplified formula. To evaluate the recombination rate plotted in Fig. 5, we have considered the initial ground state of C^+ and made the summation over the all possible final states of neutral C, up to the quantum number $n = 6$. This example shows a recombination rate smaller than the ionization one by several orders of magnitude. This result can be understood using detailed balance: in the plasma conditions where the radiative acceleration due to ion A^i is important, both ions A^i and A^{i+1} are significantly populated. In this case, the recombination rate is much smaller than the ionization one since the occupation of the states causing most ionizations (highly excited states of A^i) is much smaller than that which recombines (the ground state of A^{i+1}).

References

Alecian G., 1994, A&A 289, 885
Alecian G., Michaud G., 1981, ApJ 245, 226
Alecian G., Artru M.-C., 1990, A&A 234, 323
Alecian G., Michaud G., Tully J., 1993, ApJ 411, 882
Anders E., Grevesse N., 1989, Geochimica et Cosmochimica Acta 53, 197
Babel J., Michaud G., 1991, A&A 248, 155
Borsenberger J., Michaud G., Praderie F., 1979, A&A 76, 287
Borsenberger J., Praderie F., Michaud G., 1981, ApJ 243, 533
Burgers J. M., 1969, Flow Equations for Composite Gases. Academic Press, New York
Butler K., Mendoza C., Zeippen C. J., 1993, J. Phys. B, in press
Chapman S., Cowling T. G., 1970, The Mathematical Theory of Non-uniform Gases, 3rd ed. Cambridge Univ. Press, Cambridge
Clausset F., Stehlé C., Artru M.-C., 1994, A&A 287, 666
Cowan R. D., 1981, The Theory of Atomic Structure and Spectra. Univ. of California Press, Berkeley, p. 404
Cox A. N., 1965, Stellar Structure. In Aller L. H., McLaughlin D. B. (eds.) Stars and Stellar Systems, vol. 8. University of Chicago Press, Chicago, p. 218
Cox A. N., 1977, private communication
Cunto W., Mendoza C., Ochsenbein F., Zeippen C. J., 1993a, Bull. Inform. CDS 42, 39
Cunto W., Mendoza C., Ochsenbein F., Zeippen C. J., 1993b, A&A 275, L5
Dimitrijević M. S., Konjević N., 1980, J. Quant. Rad. Transfer 24, 451
Dimitrijević M. S., Konjević N., 1986, A&A 163, 297
Dimitrijević M. S., Konjević N., 1987, A&A 172, 345
Dworetsky M. M., Castelli F., Faraggiana R. (eds.), 1993, Peculiar versus Normal Phenomena in A-type and Related Stars, Proc. IAU Coll. 138, PASPC 44
Fernley J. A., Taylor K. T., Seaton M. J., 1987, J. Phys. B 20, 6457
Gonzalez J.-F., Artru M.-C., Michaud G., 1994, in preparation
Grevesse N., Noels A., 1993, in Prantzos N., Vangioni-Flam E., Cassé M. (eds.) Origin and Evolution of the Elements. Cambridge Univ. Press, Cambridge, p. 15
Griem H. R., 1960, ApJ 132, 883
Griem H. R., 1968, Phys. Rev. 165, 258
Griem H. R., Baranger M., Kolb A. C., Oertel G., 1962, Phys. Rev. 125, 177
Hannaford P., Lowe R. M., Grevesse N., Noels A., 1992, A&A 259, 301
Hansen J.-P., 1980, Statistical Mechanics of Dense Plasmas. In: Balian G., Adam J.-C. (eds.) Laser-Plasma Interaction, Les Houches, Session XXXIV. North-Holland Publishing Co., Amsterdam
Hummer D. G., Mihalas D., 1988, ApJ 331, 794
Iglesias C. A., Rogers F. J., Wilson B. G., 1992, ApJ 397, 717
Jefferies J., 1968, Spectral Line Formation. Blaisdel, Waltham, Mass.
Kurucz R. L., 1979, ApJS 40, 1
Kurucz R. L., 1990, Transactions of the International Astronomical Union XXB, 168
Kurucz R. L., 1991, in Crivelari L., Hubeny I., Hummer D. G. (eds.) Stellar Atmospheres: Beyond Classical Models. Kluwer, Dordrecht, p. 441
LeBlanc F., Michaud G., 1993, ApJ 408, 251
LeBlanc F., Michaud G., 1994, submitted to A&A
Luo D., Pradhan A. K., 1989, J. Phys. B 22, 3377
Massacrier G., 1994, in preparation
Michaud G., 1970, ApJ 160, 641
Michaud G., 1987, Physica Scipta 36, 112
Michaud G., 1993, Physica Scipta T47, 143
Michaud G., Proffitt C., 1993, in Weiss W. W., Baglin A. (eds.) Inside the Stars, Proc. IAU Coll. 137, PASPC 40, 246

© European Southern Observatory • Provided by the NASA Astrophysics Data System

1995A&A...297..223G

Michaud G., Tutukov A. (eds.), 1991, Evolution of Stars: the Photospheric Abundance Connection, Proc. IAU Symp. 145, Kluwer Ac. Press
Michaud G., Charland Y., Vauclair S., Vauclair G., 1976, ApJ 210, 447
Michaud G., Martel A., Ratel A., 1978, ApJ 226, 48
Michaud G., Montmerle T., Cox A. N., et al., 1979, ApJ 234, 206
Michaud G., Vauclair G., Vauclair S., 1983, ApJ 267, 256
Mihalas D., 1978, Stellar Atmospheres, 2nd ed. Freeman, San Francisco
Montmerle T., Michaud G., 1976, ApJS 31, 489
Paquette C., Pelletier C., Fontaine G., Michaud G., 1986, ApJS 61, 197
Peach G., Saraph H. E., Seaton M. J., 1988, J. Phys. B 21, 3669
Radzig A. A., Smirnov B. M., 1985, Reference Data on Atoms, Molecules, and Ions. Springer-Verlag, Berlin
Ratel A., 1975, Internal Report, Univ. de Montréal
Richer J., Michaud G., 1993, ApJ 416, 312
Rogers F. J., Iglesias C. A., 1992, ApJS 79, 507
Seaton M. J., 1962, in Bates D. R. (ed.) Atomic and Molecular Processes. Academic Press, New-York
Seaton M. J., 1987, J. Phys. B 20, 6363
Seaton M. J., Zeippen C. J., Tully J. A. et al., 1992, Rev. Mexicana Astron. Astrof. 23, 19
Seaton M. J., Yan Y., Mihalas D., Pradhan A. K., 1994, MNRAS 266, 805
Sobelman I. I., Vainshtein L. A., Yukov E. A., 1981, Excitation of Atoms and Broadening of Spectral Lines. Springer-Verlag, Berlin
Sommerfeld A., 1939, Atombau und Spektrallinien, vol. 2, 5th ed., Braunschweig
Spitzer L., 1968, Stars and Stellar Systems, vol. 7. Univ. of Chicago Press, Chicago, p. 94
Stelhé C., 1994, private communication
Tully J. A., Seaton M. J., Berrington K. A., 1990, J. Phys. B 23, 3811
Turcotte S., Richer J., Michaud G., 1994, in preparation
Vauclair S., Hardorp J., Peterson D., 1979, ApJ 227, 526

This article was processed by the author using Springer-Verlag LaTeX A&A style file version 3.

© European Southern Observatory • Provided by the NASA Astrophysics Data System